MATERIALS CHEMISTRY FRONTIERS

Stimuli Responsive Furan and Thiophene Substituted Difluoroboron β-Diketonate Materials

Journal:	*Materials Chemistry Frontiers*
Manuscript ID	QM-RES-04-2016-000008.R1
Article Type:	Research Article
Date Submitted by the Author:	09-May-2016
Complete List of Authors:	Morris, William; University of Virginia, Department of Chemistry Butler, Tristan; University of Virginia, Department of Chemistry Kolpaczynska, Milena; University of Virginia, Department of Chemistry Fraser, Cassandra; University of Virginia, Department of Chemistry

Stimuli Responsive Furan and Thiophene Substituted Difluoroboron β-Diketonate Materials

*William A. Morris, Tristan Butler, Milena Kolpaczynska, Cassandra L. Fraser**

Department of Chemistry, University of Virginia, Charlottesville, Virginia 22904

*Corresponding author: fraser@virginia.edu

Keywords: β-diketonate, difluoroboron, mechanochromic luminescence, solid-state emission, fluorescence lifetime, reversible thermally responsive emission.

Abstract

Difluoroboron β-diketonate (BF_2bdk) compounds exhibit solid-state switchable luminescence under excitation by UV light. This property is usually manifested as a blue-shift in emission when dye films are thermally annealed followed by a red-shift in response to mechanical shear (i.e. mechanochromic luminescence). Here we report thiophene and furan heterocycle-substituted dyes bearing short methoxy and long dodecyloxy chain substituents. Optical properties of the dyes were investigated in solution, pristine powders, and films on paper and glass. The structural and thermal properties of the dyes were also investigated by powder x-ray diffraction (XRD) and differential scanning calorimetry (DSC), respectively. The methoxy-substituted dyes exhibited neither thermal nor mechano-responsive behavior, however, addition of a longer C_{12} alkoxyl chain substituent resulted in stimuli-responsive behavior. The furan and thiophene dodecyloxy-substituted dyes both exhibit high-contrast reversible luminescence switching between crystalline, blue-shifted and amorphous red-shifted emissive states. For the furan dye, gentle heating produced a green emissive form while melting followed by rapid cooling produced an orange emissive form. The thiophene dye, on the other hand, exhibited blue-shifted emission when annealed below its melting temperature and red-shifted emission when smeared with a cotton swab (mechanochromic luminescence). These transformations for both dyes were found to be completely reversible, making them potential candidates for applications requiring reusable, functional materials.

Introduction

Tetracoordinate boron complexes are receiving much attention for their attractive optical properties and high stability compared to tri-coordinate boron species.[1,2] Difluoroboron β-diketonate (BF_2bdk) complexes are of particular interest due to their impressive emission properties and the facile synthesis of β-diketonates *via* Claisen condensation from a variety of commercially available ketones and esters.[1,3-7] Desirable properties of BF_2bdks include high extinction coefficients,[8-10] high quantum yields,[8-10] two-photon absorption cross-sections,[8,11] a range of emission colors in solution and the solid state,[10,12] solvatochromism,[4] and the ability to impart significant intramolecular charge transfer (ICT) character in unsymmetrical analogues.[13] Previously we reported the unique mechanochromic luminescent (ML) properties[6,7,12,14,15] of BF_2bdk dyes as well as their ability to act as dual-emissive ratiometric oxygen sensors in polymer media.[3,16-19] Mechanoluminescence in these dyes involves switching between a short-wavelength (blue-shifted) ordered emissive state and long-wavelength (red-shifted) amorphous emissive state. The former is accessible via thermal annealing and the latter, by applying shear force to the annealed material.[14] Exciton migration to lower energy emitting H-aggregates in the amorphous state is believed to be responsible for the red-shift in fluorescence observed upon smearing.[20] Substituents attached to the bdk ligand, such as halides[7,21] or alkoxyl chains of varying length,[6] are also known to affect ML properties. Aryl substituted BF_2bdks with donor-acceptor motifs typically exhibit high-contrast, reversible ML.[12,14,22]

Heteroaromatic systems with impressive optical properties are abundant. As reported by Rasmussen and coworkers, oligothiophene materials have high quantum

yields as well as significant solid-state emission.[23,24] End-capping DTP oligomers with thienyl groups produced red-shifted absorption and emission maxima in comparison to phenyl end-caps.[23] Yam *et al.* have synthesized a functional material capable of memory storage utilizing a ternary logic state by combining benzothiadiazole and BF_2bdk moieties. This material derives its unique capabilities from charge transfer between the benzothiadiazole and BF_2bdk moieties.[25] More recently, Kato and coworkers have demonstrated liquid crystalline materials based on oligothiophenes exhibiting tunable, reversible shear-induced ML.[26] Oxygen heteroaromatic materials also show responsive behavior. Greco *et al.* have reported reversible temperature dependent emission in solution of furan-containing nucleosides.[27] Naeem *et al.* have synthesized stimuli-responsive anthracene-benzoxazole (ABO) and antrhacene-thiazole (ABT) compounds in which the anthracene acts as an electron donor and the benzoxazole or thiazole moieties act as electron acceptors. The ABO dye exhibited stable ML while the ABT dye recovered mechanically-induced emission changes almost instantly. The differences in behavior were ascribed to the heteroatoms (i.e. oxygen vs sulfur).[28]

Kim and coworkers have recently reported diketopyrrolopyrrole (DPP) derivatives showing mechanical and thermally responsive emissive behavior. They found that the aforementioned properties were also heavily influenced by the length of alkyl chain substituents. In particular, a DPP derivative bearing a C_8H_{17} chain (DPP8) could access a stable, supercooled liquid state with characteristic low quantum yield red emission. Once in this state, the material was stable despite subsequent thermal treatment. However, a change to the crystalline, high quantum yield, blue-shifted emissive state could be brought about *via* mechanical shear force creating sufficiently large nucleation

sites. They attributed this to an extremely small ΔG between the red emitting, supercooled liquid and the yellow emitting crystalline solid. The C_8H_{17} substituent afforded this unique functionality while other shorter and longer chains did not. This further demonstrates that the length of an alkyl chain substituent can have substantial effects on thermal properties.[29]

In this study, four compounds were synthesized in order to probe the consequences of replacing one of the aryl moieties in BF_2bdks dyes with either a thiophene or furan heterocycle (Figure 1). Based on previous work, we reasoned that thiophene and furan heterocycles might bring about more red-shifted emissions with high quantum yields.[23] In fact, a recent study by Kolpaczynska *et al.* revealed that thiophene-substituted BF_2bdks displayed red-shifted room temperature phosphorescence (RTP) in a polylactic acid (PLA) matrix.[19] To probe alkyl chain length effects, methoxy and dodecyloxy substituents were attached to the 4-positions of the phenyl rings. The optical properties of the dyes were studied in CH_2Cl_2 solution as well as in the solid state as both films on weighing paper and thinner films on glass substrates. Density Functional Theory (DFT) calculations were performed to model the HOMO and LUMO molecular orbital (MO) diagrams and the absorption spectra in CH_2Cl_2 solution. Specifically, BF_2tbmOMe and BF_2fbmOMe dyes as well as BF_2tbmOC3 were explored in order to simulate the effects of chain lengths beyond CH_3 on solution optical properties. Pristine powders were studied using differential scanning calorimetry (DSC) to detect thermally induced phase transitions. Powder X-ray diffraction (XRD) analytical techniques were used on both pristine powders and films on glass to gauge the crystallinity of various states. Thermally responsive properties were also investigated.

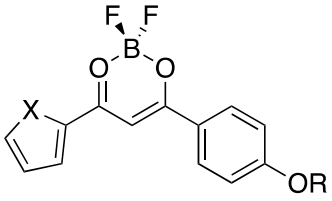

BF_2tbmOMe: X = S, R = CH_3
BF_2tbmOC12: X = S, R = $C_{12}H_{25}$
BF_2fbmOMe: X = O, R = CH_3
BF_2fbmOC12: X = O, R = $C_{12}H_{25}$

Figure 1. Chemical structures of thiophene and furan substituted dyes.

Experimental Methods

Materials

Solvents THF and CH_2Cl_2 were dried over 3 Å molecular sieves activated at 300 °C as previously described.[30] Reactions were monitored using silica TLC plates. Compounds purchased from Sigma-Aldrich were reagent grade and used without further purification. Methyl 4-dodecyloxybenzoate[31] and thiophene-substituted dyes[19] were synthesized by a previously reported method. Additional synthetic details are provided in the electronic supporting information (ESI).

Methods

^{1}H NMR (600 MHz) spectra were recorded in dilute $CDCl_3$ solvent using a Varian VRMS/600 instrument. Spectra were referenced to the signals for residual protio-$CDCl_3$ at 7.26 ppm and coupling constants were reported in Hz. Mass spectra were recorded using a Micromass Q-TOF Ultima spectrometer using electrospray ionization (ESI) MS techniques. UV-vis spectra were collected on a Hewlett-Packard 8452A diode-array spectrophotometer. Steady-state fluorescence emission spectra were obtained on a Horiba Fluorolog-3 Model FL3-22 spectrofluorometer (double-grating excitation and

double-grating emission monochromator). Time-correlated single-photon counting (TCSPC) fluorescence lifetime measurements were performed with a NanoLED-370 (λ_{ex} = 369 nm) excitation source and a DataStation Hub as the SPC controller. Lifetime data were analyzed with DataStation v2.4 software from Horiba Jobin Yvon. Fluorescence quantum yields, Φ_F, in CH_2Cl_2 were calculated *versus* a dilute anthracene solution in ethanol as a standard using a previously described method[32] and the following values: Φ_F anthracene in ethanol = 0.27[33], n_D^{20} ethanol = 1.36, n_D^{20} CH_2Cl_2 = 1.424. Optically dilute CH_2Cl_2 solutions of all samples were prepared in 1 cm path length quartz cuvettes with absorbances <0.1 (a.u.). Powder XRD patterns were obtained using a Panalytical X'Pert Pro MPD diffractometer operating at 40kV and 40ma using Cu Kα radiation. DSC was performed on the pristine powders using a TA Instruments DSC 2920 Modulated DSC and data were analyzed using the Universal Analysis software V 2.3 from TA Instruments. Thermograms were recorded using the standard mode and temperature ramp rates of 5 °C/min or 10 °C/min. A conditioning cycle followed by a second heating/cooling cycle was measured for each sample.

Films on weighing paper were created by smearing a small amount of dye onto 5 x 5 cm^2 pieces of weighing paper with nitrile examination gloves. The samples were weighed to ensure a dye mass of ~1-3.5 mg spread out over the entire 5 x 5 cm^2 area. A Laurel Technologies WS-650S spin-coater was used to make the spin-cast films. The films were fabricated by preparing 10^{-2} M solutions of the dyes and applying ~5 drops of these solutions to circular microscope cover glass slides 25 mm in diameter rotating at 3000 rpm. The films were dried *in vacuo* for 15 min before further processing. Thin films for XRD analysis of BF_2fbmOC12 were fabricated by adding 10 drops of a saturated

toluene solution to 18 x 18 mm^2 square microscope cover glass slides and evaporating the solvent in air, yielding films in the green phase. Orange films were produced by heating green BF_2fbmOC12 films above the melting point with a heat gun (i.e. holding the heat source ~3 cm from the film for ~1 s) followed by rapid cooling in air at room temperature. Drop-cast films of BF_2tbmOC12 were prepared by applying ~20 drops of a 10^{-2} M solution to circular microscope cover glass slides 25 mm in diameter. The films were allowed to dry under ambient conditions and then further dried *in vacuo* for 15 min prior to performing measurements.

Results and Discussion

Optical Properties in Solution

All thiophene and furan compounds showed very similar absorptions and emissions in CH_2Cl_2 solution with absorbance maxima (λ_{abs}) in the range of 413-418 nm and peak emissions (λ_{em}) in the range of 437-445 nm (Table 1). Little variation in λ_{abs}, λ_{em}, and fluorescence lifetime (τ_F) was observed despite the difference in alkyl chain length and heteroatom substitution (Table 1, Figure S1). This is typical for this class of dyes.[6]

Density functional theory (DFT) was used to model the molecular orbital (MO) diagrams and the absorption spectra in CH_2Cl_2 solution of BF_2tbmOMe and BF_2fbmOMe as well as a compound bearing a C_3H_7 chain (BF_2tbmOC3) to simulate alkyl chain lengths beyond three carbons (Figure 2, Table S3, Table S4). The computed absorption spectra reveal the strongest transitions to be from the highest occupied molecular orbital (HOMO) to the lowest unoccupied molecular orbital (LUMO) for all three dyes. Furthermore, these transitions are predominantly π-π^* in character, as expected from the

experimental data. In the past, the solution properties of BF_2bdks have proved to be relatively insensitive to alkyl chain length,[6] consistent with the fact that amplitude in the HOMOs and LUMOs does not extend past the first carbon in the alkyl chain. With the exception of BF_2tbmOC12 (Φ_F = 0.71), all other derivatives showed modest fluorescent quantum yields (Φ_F) ranging from Φ_F = 0.35 for BF_2fbmOMe, to Φ_F = 0.48 for BF_2fbmOC12.

A trend can be established based on alkyl chain length, as $C_{12}H_{25}$ derivatives possess higher Φ_F relative to their methoxy-substituted counterparts. An increase in Φ_F when going from methoxy to dodecyloxy chains has been previously observed for BF_2dibenzoylmethane (BF_2dbm) derivatives.[6]

Table 1. Optical Properties of Heterocycle-Substituted BF_2bdks in CH_2Cl_2.

Dye	λ_{abs} [a] (nm)	ε [b] (M^{-1} cm^{-1})	λ_{em} [c] (nm)	τ_F [d] (ns)	Φ_F [e]
BF_2tbmOMe	417	56,000	445	2.06	0.38
BF_2tbmOC12	418	62,000	441	2.08	0.71
BF_2fbmOMe	413	28,000	437	1.93	0.35
BF_2fbmOC12	415	65,000	439	1.92	0.48

[a]Absorption maxima.
[b]Extinction coefficients calculated at the absorption maxima.
[c]Fluorescence emission maxima excited at 369 nm (except **1** excited at 350 nm).
[d]Fluorescence lifetime excited with a 369 nm light-emitting diode (LED) monitored at the emission maximum. All fluorescence lifetimes are fitted to single-exponential decay.
[e]Relative quantum yield, with anthracene in EtOH as a standard.

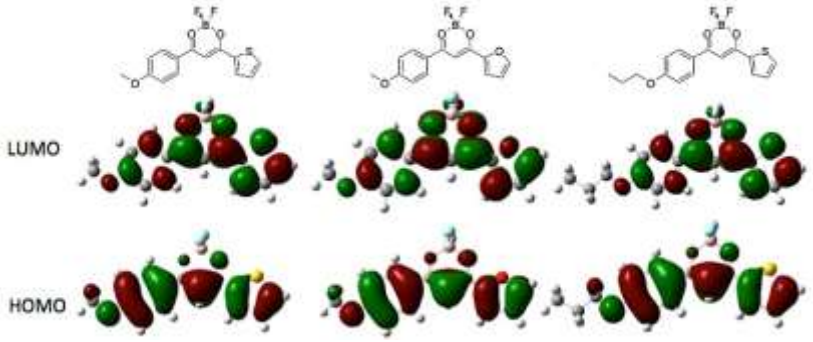

Figure 2. Molecular orbital (MO) diagrams of BF_2tbmOMe and BF_2fbmOMe as well as BF_2tbmOC_3H_7 to simulate longer chains. Their respective highest occupied molecular orbitals (HOMO) and lowest unoccupied molecular orbitals (LUMO) are displayed.

Pristine Powders

The emissions of dye pristine powders were measured under ambient conditions (Table S1, Figure 3). The OMe derivatives BF_2tbmOMe and BF_2fbmOMe show very similar broad red-shifted emission; whereas, the $C_{12}H_{25}$ derivatives show quite different emission spectra. A single short wavelength emission profile was observed for BF_2tbmOC12, while BF_2fbmOC12 showed a weak, structured blue-shifted peak similar to the thiophene-substituted counterpart and a much more intense broad red-shifted peak. Excitation spectra were monitored at the λ_{max} for the blue-shifted and red-shifted transitions. Both excitation spectra were nearly identical from 300-480 nm, suggesting that the two peaks arise from the same ground-state species (Figure S2). This may indicate that the orange emission is due to excimer formation, or energy transfer to other lower energy emitting species in the excited state.[34]

These results indicate that the identity of the heteroatom (i.e. S or O) has very little effect on the emission wavelength of pristine powders and that the dominant factor in determining the emission color is the alkyl chain length. The blue-shifted emission observed in $C_{12}H_{25}$ powders has been previously ascribed to the steric hindrance of the $C_{12}H_{25}$ chain limiting dye-dye interactions that red shift emission.[6] In methoxy-

substituted analogues, dye-dye interactions such as π-stacking and longer range effects that would red shift emission are more probable since the β-diketonate cores are closer together, undiluted by packed alkyl chain domains.[6,17] This result is analogous to a study performed by Nguyen *et al.* wherein BF_2dbm derivatives with long alkoxyl chains exhibited more blue-shifted solid-state emissions compared to shorter chain derivatives.[6]

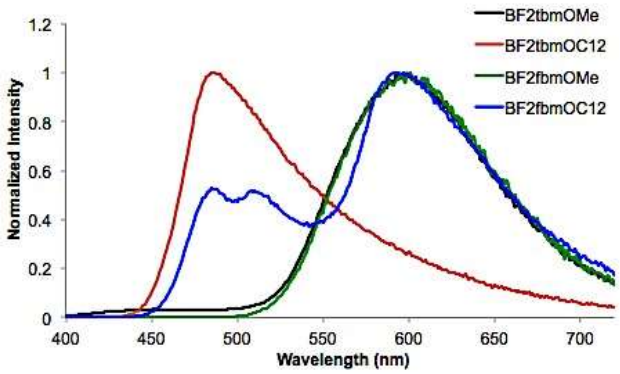

Figure 3. Emission spectra of pristine powders (λ_{ex} = 369).

Thermally Responsive Emission

In the process of testing these dyes for ML properties, it was discovered that the long chain furan dye BF_2fbmOC12 exhibited highly controllable and reversible changes in emission in response to different methods of heating while the thiophene dye BF_2tbmOC12 did not show this same behavior. The emission spectrum of the melted BF_2fbmOC12 powder was also obtained. The melted phase of BF_2fbmOC12 was accessed by heating the pristine powder above the melting point until melted (~5 sdeconds) then rapidly removing the heat source and cooling in an ice bath. The resultant melt-quenched material appeared orange to the eye and the emission spectrum showed only a single broad peak at 581 nm corresponding to the red-shifted peak in the spectrum of the dye as a pristine powder (Figure 3).

Although, this property could be observed for powders, the effect was much more accessible and reversible with films of the material. When the dye was initially smeared into a film on weighing paper and subjected to UV illumination, it was evident that the film represented a heterogeneous mixture of emissive states, one being blue-shifted (λ_{em} = ~470 nm), and the other being red-shifted (λ_{em} = 587 nm) and this was corroborated by an emission spectrum of the as-smeared (ASM) dye. If the film was gently heated for five seconds (e.g. with a heat gun from approximately one foot away), a homogenous film with green emission (λ_{em} = 519 nm) could be obtained. Heating for one minute in an oven at 125 °C (just below the melting point of 127 °C) produced the same results. The orange emissive state, on the other hand, was accessible *via* a different method of thermal processing, namely melt quenching. Intense heat sufficient to melt the film was applied (e.g. with a heat gun by holding the heat source approximately one inch from the film). When the heat source was removed rapidly and the film cooled quickly in the air, a homogenous, orange emitting film (λ_{em} = 575 nm) was obtained. This state is not achieved if the dye is allowed to cool slowly on a heat conductive surface, such as a laboratory bench top. Instead, under these circumstances, the warm surface provides the gentle heating necessary to access the green emissive state. The orange emissive state was also obtained by submersion of the hot film in liquid N_2 which provided sufficiently rapid cooling. Regardless of how the orange state was achieved, the transformation between orange and green emissive states was found to be completely reversible. By cycling back and forth between gentle heating and melt quenching in air, the dye could be carried through seven cycles with no deterioration in responsiveness. Given that a furan functional group is present in this dye, the heat-induced transition could be due to a

Diels-Alder cycloaddition.[35] To test this possibility, material from both the orange and green forms were re-dissolved and subjected to UV-Vis (Figure S3) and ^{1}H NMR spectral analysis. These analyses suggested that the green and orange-emitting chemical species are identical in terms of chemical composition, inconsistent with formation of a Diels Alder adduct in one and not the other. Therefore, data are consistent with a thermally induced physical change, not a chemical change.

Like other BF_2bdk dye materials, the relatively blue-shifted BF_2fbmOC12 dye film may represent a thermodynamically stable, ordered emissive state while the more red-shifted film represents a kinetically accessible, metastable, amorphous emissive state. In addition, lifetimes were recorded for films in both orange and green states (Table S2). The orange form had a significantly longer τ_{pw0} (7.61 ns) when compared to the green form (τ_{pw0} = 0.80 ns). This behavior is very similar to other BF_2bdk materials exhibiting ML,[14,15,20,31] only this time the amorphous, metastable emissive state is accessible *via* heat instead of mechanical perturbation.

Through experimentation, we were able to discover an immediate potential use of this dye for thermal printing.[36] By heating a metal object, applying it to the annealed green dye film, removing it and then quickly cooling by submersion in liquid N_2, clear images could be printed (Figure 4). Since this transformation is reversible, the process can be repeated many times on a single film. Alternative substrates for thermal printing are desirable because many papers currently used contain bisphenol A (BPA), which is potentially hazardous to human health.[37] In terms of industrial applications, this material could be used in any process that requires heating to high temperature followed by rapid cooling. Such an example of a potential application could be in the frozen food industry,

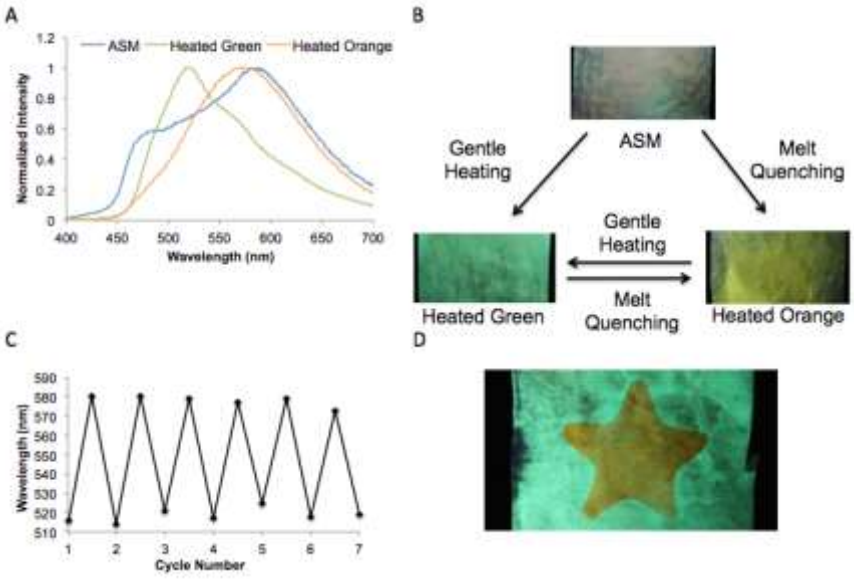

Figure 4. Demonstration of the thermally responsive emission for BF_2fbmOC12. A) Spectra of the dye film in the as-smeared (ASM), heated green, and heated orange states. B) Photographs of the dye film in all three states. C) Reversibility of the thermally responsive emissive behavior through seven gentle heating and melt quenching cycles. D) Thermal printing. A metal star was heated, pressed onto the green film for ~1 second then removed. The film was then quickly submerged in liquid N_2 to achieve the image.

where many products need to be cooked and then frozen quickly to avoid the formation of large ice crystals, which can damage the product.[38] If the dye film were encapsulated in a clear, heat-conductive container attached to the product, it could be used as a quick, easy indicator of quality control.

Interestingly, the BF_2fbmOC12 dye did not exhibit the same thermally responsive, reversible changes in emission properties as a spin-cast film on glass. The AS film was found to have red emission (λ_{em} = 597 nm) with a long τ_{pw0} under UV illumination (Figure 5, Table S2). Whether the film was gently heated with a heat gun or annealed in an oven, only a red, long-lifetime emission remained and the green emissive state could not be obtained. Therefore, it appears that spin casting locks this dye into a red-shifted

emissive state. This is likely a processing or thickness effect that, at this time, we are unable to explain. However, it was possible to fabricate thermally responsive films of the BF_2fbmOC12 dye on glass by drop-casting from a saturated toluene solution. Slow evaporation yielded a glass film of BF_2fbmOC12 in the green phase (λ_{em} = 512 nm) and the orange phase (λ_{em} = 551 nm) was produced through the melting and room temperature cooling of the green thin films using a heat gun in the same way as the films on weighing paper (Figure 5).

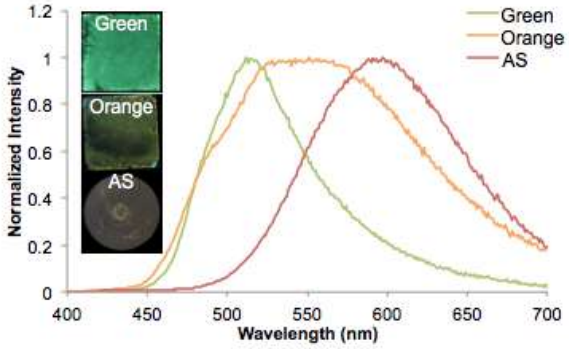

Figure 5. Emission of BF_2fbmOC12 as films on glass. Drop-cast films on glass from toluene solutions in both green and orange forms are compared to a spin-cast film from CH_2Cl_2 solution (AS = as spun).

Curiously, the $C_{12}H_{25}$ derivative of the furan-substituted dye exhibited stimuli responsive solid-state emission while the methoxy-substituted counterpart did not have this property. A previous study has shown that incorporation of an alkoxyl chain longer than OCH_3 into difluoroboron dibenzoylmethane (dbm) fluorophores can grant ML properties.[6] Perhaps the ability of the alkoxyl chains to break up closer intermolecular π-π interactions creates a greater variety of available states that may be accessed through different processing methods. In this example and others[39-41], the addition of long alkoxyl chain substituents to solid-state emitting fluorophores is an effective strategy for

imparting switchable luminescence behavior. Both Yang *et al.*[41] and Xu *et al.*[40] have both reported organic molecules with mechanically switchable emissive behavior in the solid state brought about by the addition of long aliphatic chains. They proposed, with emission and x-ray diffraction data, that the alkyl chains disrupt close supramolecular interactions such as π-π stacking. They believe this balancing of π-π and aliphatic interactions can create multiple emissive states and thus impart switchable emissive behavior.[40]

Differential Scanning Calorimetry

The dyes BF_2tbmOC12 and BF_2fbmOC12 show thermally responsive emission whereas their methoxy-substituted counterparts do not. The differences between these samples and the nature of the thermally accessible green and orange states of BF_2fbmOC12 were investigated using differential scanning calorimetry (DSC). Samples were heated above their melting points and cooled to 0 °C at a constant ramp rate (5 °C/min or 10 °C/min).

The thermal properties were reported using thermograms of the second heating/cooling cycle of each compound (Table 2, Figure S4). The melting points of methoxy-substituted BF_2tbmOMe (265.9 °C) and BF_2fbmOMe (216.5 °C) were higher compared to their alkoxylated counterparts BF_2tbmOC12 (137.0 °C) and BF_2fbmOC12 (127.7 °C). The diminished melting points observed in $C_{12}H_{25}$ samples is further evidence that the alkoxyl chains are capable of disrupting stronger intermolecular interactions. In general, thiophene dyes had slightly higher melting points than furan dyes, but the alkoxyl chain length, by far, had the greatest effect on melting temperature.

In order to investigate transformations in BF_2fbmOC12 brought about by heat, the DSC thermograms of the first heating cycle of both the green and orange powders with a constant ramp rate (10 °C /min) were compared (Figure 6). Because BF_2tbmOC12 does not respond to heat in the same way as BF_2fbmOC12, only the thermal properties of BF_2fbmOC12 were studied in depth. When the green form of BF_2fbmOC12 was heated only the melting point was observed at 127 °C, but an additional crystallization peak at 56.2 °C was observed when the orange form was heated. Chujo and coworkers have reported similar behavior for powders of difluoroboron β-diiminates in crystalline and amorphous emissive forms.[42] This is further evidence that the orange form represents an amorphous, metastable state while the green form represents a thermodynamically stable, crystalline state.

Table 2. Differential Scanning Calorimetry (DSC) Data for Pristine Dyes.[a]

	T_m[b] (°C)	ΔH[c] (kJ/mol)	T_c[b] (°C)	ΔH[c] (kJ/mol)
BF_2tbmOMe	265.9	65.0	197.2	61.3
BF_2tbmOC12	137.0	505.7	111.8	515.6
BF_2fbmOMe	216.5	142.3	163.0	101.1
BF_2fbmOC12	127.7	526.2	103.4	520.9

[a] All data was taken from the 2nd cycle.
[b] Melting point given in °C as the peak of the major endothermic transition.
[c] Enthalpy of the transition given in kJ/mol.
[d] Crystallization point given in °C as the peak of the major exothermic transition.

However, one question remains. Why does the furan-substituted derivative exhibit this thermally responsive switchable behavior while the thiophene-substituted dye does not? The answer may be found in comparing π-stacking energies and intermolecular

interactions. According to a computational study performed by Huber *et al.*, furan forms a slightly closer and stronger π-stacking interaction with benzene than thiophene due to the smaller size of the oxygen atom compared to sulfur.[43] Furthermore, it stands to reason that the stronger hydrogen bonding affinity afforded by the oxygen atom could also contribute to closer interactions between molecules. If the furan-substituted dye molecules interact with each other strongly in the H-aggregates present in the amorphous form,[20] a larger energy barrier would have to be overcome to switch from the amorphous to the crystalline emissive form. This could explain why the films and powders of BF_2fbmOC12 become trapped in the amorphous phase when their melts are rapidly quenched. The answer could also lie in the favorability of the ordered emissive state over the amorphous state for the BF_2tbmOC12 dye. The pristine powder of this dye showed preference for the ordered emissive, blue state and could not be easily converted to the amorphous phase like its furan counterpart. Also the melting point of the BF_2tbmOC12 dye pristine powder (always in the blue form) is higher than that of the furan dye, suggesting a greater degree of stability.

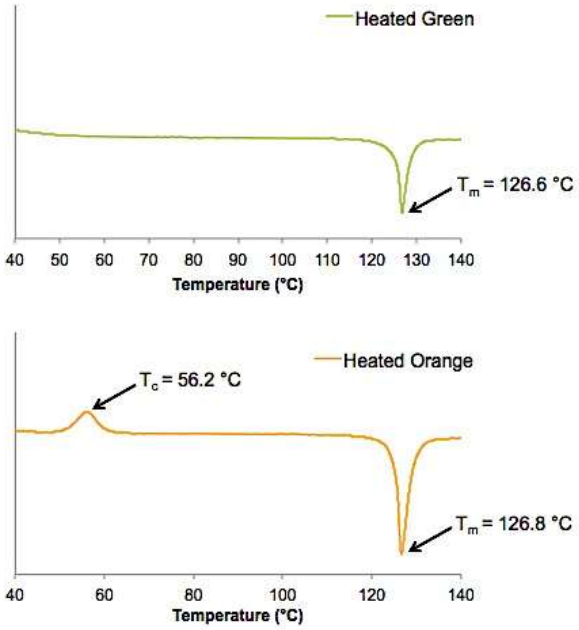

Figure 6. DSC thermograms of the first heating cycles of BF_2fbmOC12 powder in both heated green (top) and heated orange (bottom) forms. Enthalpy values (ΔH) were calculated for the transitions of the heated orange sample and are as follows: T_C (56.2 °C) = 174.8 kJ/mol, T_m (126.8 °C) = 641.4 kJ/mol.

Mechanochromic Luminescence

Although BF_2fbmOC12 showed excellent responsiveness to heating, this dye and both methoxy-substituted dyes did not exhibit the ML properties typical for many BF_2bdks.[6,7,14] However, BF_2tbmOC12 did possess ML properties. While BF_2bdks exhibit a degree of mechano-responsiveness as bulk powders, that can be activated by prolonged grinding, this property is greatly amplified when the dye materials are fabricated as films.[6,7,14,22,31] Therefore the dye was fabricated into both thin films on glass substrates and thicker films on weighing paper substrates. When the BF_2tbmOC12 dye weighing paper film is annealed for ten minutes at 130 °C (below the melting temperature of 137 °C), it exhibits blue emission and the spectrum reveals a relatively narrow peak (485 nm) (Figure 7). When the thermally annealed (TA) film is smeared with a cotton swab, the

emission changes to yellow and the spectrum reveals a much broader red-shifted peak (562 nm). This 77 nm shift in emission after smearing represents a high contrast ML material. Furthermore, the ML property is highly reversible. A process of annealing a film at 130 °C for a minute and then smearing was repeated seven times without any noticeable decline in responsiveness. This excellent reversibility could make this dye useful in many applications in which force responsiveness is required.

To test for thickness and substrate effects, spin-cast films of BF_2tbmOC12 on glass were also fabricated. The process by which spin-cast films are fabricated allow for much thinner films than can be achieved by smearing dye powders onto paper substrates. In the past, we have observed that thinner spin-cast films on glass display slightly different properties than films on weighing paper. The most prominent of these differences is more blue-shifted and narrow fluorescence emission spectra for annealed spin-cast films *versus* films on weighing paper.[7] Immediately after spin-casting, it could be seen that the as-spun (AS) state was unique and unlike what was observed for both the TA and SM states on weighing paper substrate (Figure 8). In the case of BF_2tbmOC12, no major differences in solid-state emission properties were observed between thin spin-cast films and thicker films on weighing paper, indicating that this dye is less sensitive to thickness and substrate effects than other BF_2bdk materials.[7] The AS form seems to represent a combination of the blue and red emissive states, similar to other BF_2bdk dye films exhibiting ML, but here there is a large gap in the peak emissions of the TA and SM forms.[7] Lifetime measurements were also performed on spin-cast films in all three forms (Table S2). As is typical for BF_2bdk dyes, the red-shifted, SM emission had a much longer lifetime (τ_{pw0} = 12.12 ns) than the TA emission (τ_{pw0} = 7.03 ns). This, along

with the broadening of the peak upon smearing, suggests the formation of excimeric or unique ground-state species.[7,20,22]

Just as with furan derivatives, the thiophene dye substituted with $OC_{12}H_{25}$ exhibited switchable emissions in the solid state while its methoxy-substituted counterpart did not. This is presumably due to the disruption of close supramolecular interactions.

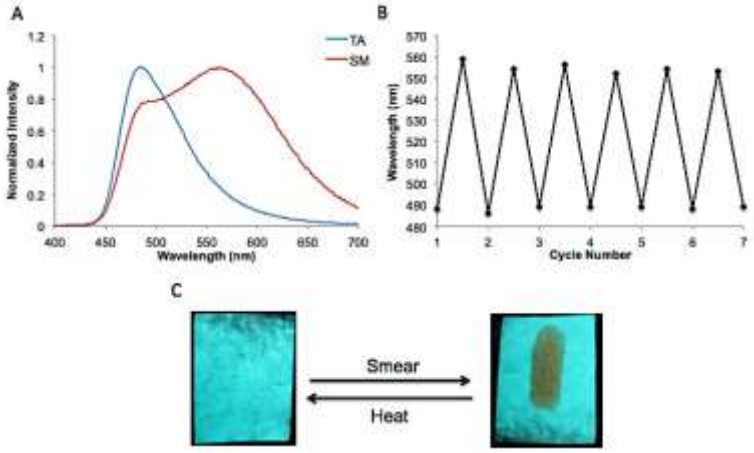

Figure 7. Mechanochromic luminescence of BF_2tbmOC12 on weighing paper: A) Emission spectra in thermally annealed (TA) and smeared (SM) states. B) Reversibility of the ML through annealing and smearing cycles. C) Photographs of films after thermal annealing (left) and smearing (right).

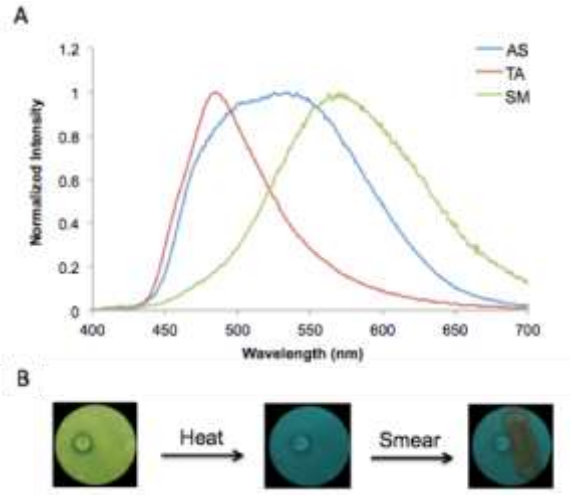

Figure 8. Mechanochromic luminescence of BF_2tbmOC12 as spin-cast films on glass. A) Emission spectra of the dye film in the as-spun (AS), thermally annealed (TA), and smeared (SM) states. B) Photographs of a film in AS, TA and SM states.

X-ray Diffraction of Films

X-ray diffraction (XRD) diffractograms were obtained for pristine powders of the BF_2tbmOC12 and BF_2fbmOC12 dyes and compared to those of the drop cast films on microscope cover glass in various forms in order to glean information about the amorphous *versus* crystalline states of these dyes (Figure 9). Drop-cast films of the BF_2tbmOC12 dye exhibited behavior typical of ML dye films.[7,22] There was no change between the as-cast (AC) and thermally annealed (TA) films, with both exhibiting a relatively strong peak at ~10° and a much smaller peak at ~15°. This suggests that the dye film is crystalline both in the AC and TA states. The diffractogram of the smeared film was devoid of peaks, confirming the amorphous nature of the smeared films.

In order to probe the thermally responsive behavior of BF_2fbmOC12, the powder XRD patterns of orange and green drop-cast films on glass were compared to the diffraction patterns of the pristine powder (Figure 9). No peaks were observed in the diffraction pattern of the orange film, whereas sharp peaks at ~24° and ~28° were detected in the diffraction pattern of the green film. The pattern of the pristine powder also displayed peaks near these same angles. These results indicate that the orange phase generated by melt quenching BF_2fbmOC12 is amorphous and the green phase produced *via* gentle heating of BF_2fbmOC12 is crystalline and both are likely to be present in the pristine powder, just as emission spectra and lifetime data suggest.

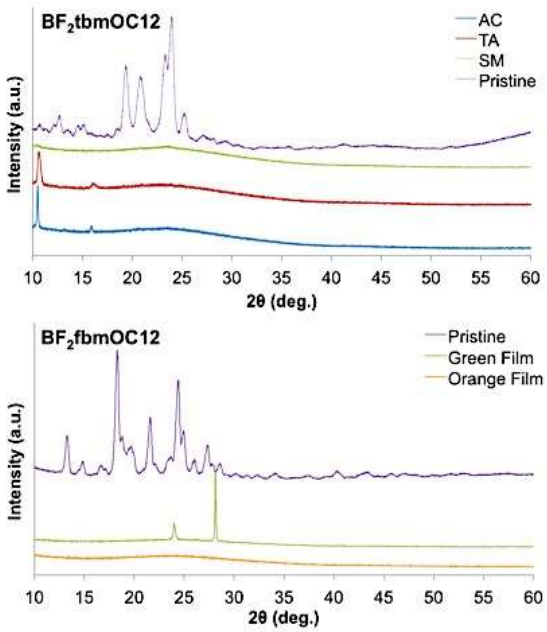

Figure 9. Powder XRD diffractograms of mechanochromic luminescent BF_2tbmOC12 samples (top) and thermally responsive BF2fbmOC12 samples (bottom). Note: The pristine powder of BF_2tbmOC12 is compared to drop-cast films in the as-cast (AC), thermally annealed (TA), and smeared (SM) states. The BF_2fbmOC12 pristine powder is compared to orange (melt quenched) and green (gentle heated) drop-cast films. BF_2fbmOC12.

Conclusion

In summary, four solid-state emissive difluoroboron β-diketonate dyes bearing thiophene and furan substituents as well as short (OMe) and long ($OC_{12}H_{25}$) alkoxyl chain substituents were synthesized. While the length of the chain had little effect on the optical properties of the dyes in solution, the $C_{12}H_{25}$ alkoxyl chain afforded both the thiophene and furan substituted dyes unique, switchable solid-state luminescence features. The BF_2tbmOC12 dye exhibited high-contrast ($\Delta\lambda_{max}$ = 77 nm) reversible ML as both films on weighing paper and glass substrates. Powder XRD revealed the blue-shifted, thermally annealed (TA) form of the dye to be crystalline in nature while the red-

shifted, smeared (SM) form was amorphous. Furthermore, this dye could be carried through at least seven cycles of annealing and smearing without any noticeable deterioration in the responsiveness.

The BF_2fbmOC12 dye showed similar dual emissive behavior as films on glass or weighing paper, but the stimulus required for switching of emission was different. By gently heating the sample a green emissive form could be obtained. An orange emissive form could be obtained *via* melt quenching. This could be achieved by melting the film and then quickly removing the heat source, allowing the film to cool quickly either while held in the air or submerging in liquid N_2. Powder XRD of drop-cast films in both emissive forms revealed the green form to be crystalline with well-defined peaks in the diffractograms while the orange form was amorphous with no peaks. The unique responsiveness could make this dye useful as a quality control indicator for any process requiring intense heating followed by rapid cooling.

Because both dyes bearing $OC_{12}H_{25}$ alkoxyl chains exhibited switchable emissive behavior while the methoxy-substituted counterparts did not, adding a long alkyl chain substituent to π-stacking, solid-state emitting fluorophores could be an effective strategy for inducing switchable luminescent behavior. Presumably, this is due to the chains disrupting close intermolecular interactions such as π-stacking and thus creating more available molecular configurations. Finally, the difference in thermally responsive emissive behavior between BF_2tbmOC12 and BF_2fbmOC12 may be attributed to closer intermolecular interactions in the H-aggregated furan dye causing the material to become trapped in the amorphous state when it is heated to the melting point and then the melt is rapidly quenched. It may also be attributed to a much more stable ordered emissive state

of the BF_2tbmOC12 material strongly driving the transformation to the ordered emissive state.

Acknowledgements

We thank the National Science Foundation (CHE 1213915) and the National Institutes of Health (R01 CA167250) for support for this research. We thank Christopher DeRosa for assistance and helpful discussions.

Supporting Information

Additional synthetic, spectral and computational details are provided free of charge in the electronic supplementary information (ESI).

References

(1) Tanaka, K.; Chujo, Y. *NPG Asia Mater.* **2015**, *7*, e223.

(2) Tan, R.; Lin, Q.; Wen, Y.; Xiao, S.; Wang, S.; Zhang, R.; Yi, T. *Cryst. Eng. Comm.* **2015**, *17*, 6674.

(3) DeRosa, C. A.; Kerr, C.; Fan, Z.; Kolpaczynska, M.; Mathew, A. S.; Evans, R. E.; Zhang, G.; Fraser, C. L. *ACS Appl. Mater. Interfaces* **2015**, *7*, 23633.

(4) Butler, T.; Morris, W. A.; Samonina-Kosicka, J.; Fraser, C. L. *Chem. Commun.* **2015**, *51*, 3359.

(5) Mirochnik, A. G.; Bukvetskii, B. V.; Fedorenko, E. V.; Karasev, V. E. *Russ. Chem. Bull.* **2004**, *53*, 291.

(6) Nguyen, N. D.; Zhang, G.; Lu, J.; Sherman, A. E.; Fraser, C. L. *J. Mater. Chem.* **2011**, *21*, 8409.

(7) Morris, W. A.; Liu, T.; Fraser, C. L. *J. Mater. Chem. C* **2015,** 352.

(8) Cogné-Laage, E.; Allemand, J.-F.; Ruel, O.; Baudin, J.-B.; Croquette, V.; Blanchard-Desce, M.; Jullien, L. *Chem. Eur. J.* **2004**, *10*, 1445.

(9) Chow, Y. L.; Johansson, C. I.; Zhang, Y.-H.; Gautron, R.; Yang, L.; Rassat, A.; Yang, S.-Z. *J. Phys. Org. Chem.* **1996**, *9*, 7.

(10) Ono, K.; Yoshikawa, K.; Tsuji, Y.; Yamaguchi, H.; Uozumi, R.; Tomura, M.; Taga, K.; Saito, K. *Tetrahedron* **2007**, *63*, 9354.

(11) Halik, M.; Wenseleers, W.; Grasso, C.; Stellacci, F.; Zojer, E.; Barlow, S.; Bredas, J.-L.; Perry, J. W.; Marder, S. R. *Chem. Commun.* **2003**, *0*, 1490.

(12) Liu, T.; Chien, A. D.; Lu, J.; Zhang, G.; Fraser, C. L. *J. Mater. Chem.* **2011**, *21*, 8401.

(13) Xu, S.; Evans, R. E.; Liu, T.; Zhang, G.; Demas, J. N.; Trindle, C. O.; Fraser, C. L. *Inorg. Chem.* **2013**, *52*, 3597.

(14) Zhang, G.; Lu, J.; Sabat, M.; Fraser, C. L. *J. Am. Chem. Soc.* **2010**, *132*, 2160.

(15) Butler, T.; Morris, W. A.; Samonina-Kosicka, J.; Fraser, C. L. *ACS Appl. Mater. Interfaces* **2016**.

(16) Zhang, G.; Palmer, G. M.; Dewhirst, M. W.; Fraser, C. L. *Nat. Mater.* **2009**, *8*, 747.

(17) Samonina-Kosicka, J.; DeRosa, C. A.; Morris, W. A.; Fan, Z.; Fraser, C. L. *Macromolecules* **2014**, *47*, 3736.

(18) DeRosa, C. A.; Samonina-Kosicka, J.; Fan, Z.; Hendargo, H. C.; Weitzel, D. H.; Palmer, G. M.; Fraser, C. L. *Macromolecules* **2015**, *48*, 2967.

(19) Kolpaczynska, M.; DeRosa, C. A.; Morris, W. A.; Fraser, C. L. *Aust. J. Chem.* **2016**.

(20) Sun, X.; Zhang, X.; Li, X.; Liu, S.; Zhang, G. *J. Mater. Chem.* **2012**, *22*, 17332.

(21) Yoshii, R.; Suenaga, K.; Tanaka, K.; Chujo, Y. *Chem. Eur. J.* **2015**, 4506.

(22) Nguyen, N. D.; Zhang, G.-Q.; Lu, J.-W.; Sherman, A. E.; Fraser, C. L. *J. Mater. Chem.* **2011**, *21*, 8409.

(23) Evenson, S. J.; Pappenfus, T. M.; Delgado, M. C. R.; Radke-Wohlers, K. R.; Navarrete, J. T. L.; Rasmussen, S. C. *Phys. Chem. Chem. Phys.* **2012**, *14*, 6101.

(24) Rasmussen, S. C.; Evenson, S. J.; McCausland, C. B. *Chem. Commun.* **2015**, *51*, 4528.

(25) Poon, C.-T.; Wu, D.; Lam, W. H.; Yam, V. W.-W. *Angew. Chem. Int. Ed.* **2015**, *54*, 10569.

(26) Mitani, M.; Ogata, S.; Yamane, S.; Yoshio, M.; Hasegawa, M.; Kato, T. *J. Mater. Chem. C* **2015**.

(27) Greco, N. J.; Tor, Y. *Tetrahedron* **2007**, *63*, 3515.

(28) Naeem, K. C.; Subhakumari, A.; Varughese, S.; Nair, V. C. *J. Mater. Chem. C* **2015**, *3*, 10225.

(29) Chung, K.; Kwon, M. S.; Leung, B. M.; Wong-Foy, A. G.; Kim, M. S.; Kim, J.; Takayama, S.; Gierschner, J.; Matzger, A. J.; Kim, J. *ACS Cent. Sci.* **2015**, *1*, 94.

(30) Williams, D. B. G.; Lawton, M. *J. Org. Chem.* **2010**, *75*, 8351.

(31) Zhang, G.; Singer, J. P.; Kooi, S. E.; Evans, R. E.; Thomas, E. L.; Fraser, C. L. *J. Mater. Chem.* **2011**, *21*, 8295.

(32) Carraway, E. R.; Demas, J. N.; DeGraff, B. A.; Bacon, J. R. *Anal. Chem.* **1991**, *63*, 337.

(33) Heller, C. A.; Henry, R. A.; McLaughlin, B. A.; Bliss, D. E. *J. Chem. Eng. Data* **1974**, *19*, 214.

(34) Sun, X. Z., Li, X.; Liu, S.; Zhang, G. *J. Mater. Chem.* **2012**, *22*, 17332.

(35) Kappe, O. C.; Murphree, S. S.; Padwa, A. *Tetrahedron* **1997**, *53*, 14179.

(36) Shibata, S.; Murasugi, K.; Kaminishi, K. *IEEE Trans. Parts, Hybrids, Packag.* **1976**, *12*, 223.

(37) Biedermann, S.; Tschudin, P.; Grob, K. *Anal. Bioanal. Chem.* **2010**, *398*, 571.

(38) Sun, D.-W. *Advances in Food Refrigeration*; Leatherhead Food RA Pub.: Leatherhead, 2001.

(39) Sase, M.; Yamaguchi, S.; Sagara, Y.; Yoshikawa, I.; Mutai, T.; Araki, K. *J. Mater. Chem.* **2011**, *21*, 8347.

(40) Zhang, X.; Chi, Z.; Xu, B.; Jiang, L.; Zhou, X.; Zhang, Y.; Liu, S.; Xu, J. *Chem. Commun.* **2012**, *48*, 10895.

(41) Liu, W.; Wang, Y.; Bu, L.; Li, J.; Sun, M.; Zhang, D.; Zheng, M.; Yang, C.; Xue, S.; Yang, W. *J. Luminesc.* **2013**, *143*, 50.

(42) Yoshii, R.; Hirose, A.; Tanaka, K.; Chujo, Y. *Chem. Eur. J.* **2014**, *20*, 8320.

(43) Huber, R. G.; Margreiter, M. A.; Fuchs, J. E.; von Grafenstein, S.; Tautermann, C. S.; Liedl, K. R.; Fox, T. *J. Chem. Inf. Model.* **2014**, *54*, 1371.

Table of Contents Text and Graphic

Changing the heteroatom from oxygen to sulfur in difluoroboron β-diketonates results in thermally and mechanically responsive luminescent materials, respectively.